

Effects of bacterial lipopolysaccharide and Shiga Toxin on induced Pluripotent Stem Cell-derived Mesenchymal Stem Cells

Daiana Martire-Greco ^{a,d,*‡}

Alejandro La Greca ^{b*}

Luis Castillo Montañez ^a

Celeste Biani ^b

Antonella Lombardi ^b

Federico Birnberg-Weiss ^a

Alessandra Norris ^b

Flavia Sacerdoti ^{c,d}

María Marta Amaral ^{c,d}

Nahuel Rodrigues-Rodriguez ^a

Jose Ramón Pittaluga ^a

Verónica Alejandra Furmento ^b

Verónica Inés Landoni ^{a,d}

Santiago Gabriel Miriuka ^{b,d}

Carlos Luzzani ^{b,d}

Gabriela Cristina Fernández ^{a,d}

^aLaboratorio de Fisiología de los Procesos Inflamatorios. Instituto de Medicina Experimental (IMEX-CONICET). Academia Nacional de Medicina, Buenos Aires, Argentina.

^bLaboratorio de Investigación Aplicada a Neurociencias (LIAN), FLENI-CONICET, Buenos Aires, Argentina.

^cLaboratorio de Fisiopatogenia, Instituto de Fisiología y Biofísica Bernardo Houssay (IFIBIO Houssay-CONICET), Departamento de Fisiología, Facultad de Medicina, Buenos Aires (Argentina).

^dConsejo Nacional de Investigaciones Científicas y Técnicas (CONICET), Buenos Aires, Argentina.

* These authors contributed equally to this work

‡ Corresponding author: daianamartire@hotmail.com

Lead Contact

Daiana Martire-Greco

Running title

iPSC-MSC response to LPS and Stx.

Competing interest

The authors declare no competing interest.

Effects of bacterial lipopolysaccharide and Shiga Toxin on induced Pluripotent Stem Cell-derived Mesenchymal Stem Cells

Daiana Martire-Greco ^{a,c*‡}, Alejandro La Greca ^{b*}, Luis Castillo Montañez ^a, Celeste Biani ^b, Antonella Lombardi ^b, Federico Birnberg-Weiss ^a, Alessandra Norris ^b, Flavia Sacerdoti ^c, María M. Amaral ^c, Nahuel Rodrigues-Rodriguez ^a, Jose R. Pittaluga ^a, Verónica Furmento ^b, Verónica Landoni ^{a,c}, Santiago G. Miriuka ^{b,c}, Carlos Luzzani ^{b,c}, Gabriela C. Fernández ^{a,c}

^aLaboratorio de Fisiología de los Procesos Inflamatorios. Instituto de Medicina Experimental (IMEX-CONICET). Academia Nacional de Medicina, Buenos Aires, Argentina. ^bLaboratorio de Investigación Aplicada a Neurociencias (LIAN), FLENI-CONICET, Buenos Aires, Argentina. ^cLaboratorio de Fisiopatología, Instituto de Fisiología y Biofísica Bernardo Houssay (IFIBIO Houssay-CONICET), Departamento de Fisiología, Facultad de Medicina, Buenos Aires (Argentina). ^dConsejo Nacional de Investigaciones Científicas y Técnicas (CONICET), Buenos Aires, Argentina. * These authors contributed equally to this work. ‡ Corresponding author: daianamartire@hotmail.com

Abstract

Background: Mesenchymal Stem Cells can be activated and respond to different bacterial toxins. Lipopolysaccharides (LPS) and Shiga Toxin (Stx) are the two main bacterial toxins present in Hemolytic Uremic Syndrome (HUS) that cause endothelial damage. In this work we aimed to study the response of iPSC-MSC to LPS and/or Stx and its effect on the restoration of injured endothelial cells.

Methods: iPSC-MSC were used as a source of mesenchymal stem cells (MSC) and Human Microvascular Endothelial Cells-1 (HMEC-1) as a source of endothelial cells. iPSC-MSC were treated or not with LPS and/or Stx. For some experiments, Conditioned Media (CM) were collected from each plate and incubated with an anti-Stx antibody to block the direct effect of Stx, or Polymyxin to block the direct effect of LPS. In CM from both treatments, anti-Stx and Polymyxin were used. Results are expressed as mean \pm S.E.M. Significant differences ($p < 0.05$) were identified using one way analysis of variance (ANOVA) and Bonferroni's Multiple comparison test.

Results: The results obtained showed that LPS induced a pro-inflammatory profile on iPSC-MSC, but not Stx, even though they expressed Gb₃ receptor. Moreover, LPS induced on iPSC-MSC an increment in migration and adhesion to gelatin substrate. Also, the addition of CM of iPSC-MSC treated with LPS+Stx, decreased the capacity of HMEC-1 to close a wound, and did not favor the formation of new tubes. Proteomic analysis of iPSC-MSC treated with LPS and/or Stx revealed specific protein secretion patterns that support many of the functional results described here.

Conclusions: In conclusion, these results suggest that iPSC-MSC activated by LPS acquired a pro-inflammatory profile that induces migration and adhesion to extracellular matrix proteins (ECM), but the combination LPS+Stx decreased the repair of endothelial damage. The importance of this work is that it provides knowledge to understand the context in which iPSC-MSC could benefit or not the restoration of tissue injury, taking into account that the inflammatory context in response to a particular bacterial toxin is relevant for iPSC-MSC immunomodulation.

Keywords: Mesenchymal Stem Cells, Endothelial injury, Shiga-toxin, Lipopolysaccharide, regeneration, Hemolytic Uremic Syndrome

1 Introduction

2 Mesenchymal Stem Cells (MSC) are mul-
3 tipotent cells associated with the treatment of
4 different pathologies due to their regenerative
5 properties, thus providing an interesting ther-
6 apeutic option for various diseases, mainly
7 those that are present in an inflammatory re-
8 sponse and tissue damage [1]. They are an
9 heterogeneous subset of stromal stem cells that
10 can be isolated from many adult tissues. How-
11 ever, isolating MSC and obtaining a consid-
12 erable number for handling often present dif-
13 ficulties. In this sense, derivation of MSC
14 from induced Pluripotent Stem Cells (iPSC) is
15 a widely accepted method that results in cells
16 that have similar properties to those obtained
17 directly from adult tissues. In this sense, our
18 group described in a previous paper a robust
19 and fast method to obtain the iPSC-MSC that
20 were used in this work [2].

21 In recent years, the use of MSC has in-
22 creased in important clinical applications [1].
23 It has been described that these cells are in-
24 volved in immune processes and participate
25 in the repair of many types of tissue injuries,
26 mainly in a paracrine fashion by secreting nu-
27 merous soluble factors [3, 4]. Also, it is widely
28 reported the capacity of MSC to migrate into
29 injured sites and to release inflammatory and
30 growth factors [5]. Some types of MSC, like
31 those obtained from bone marrow, can poten-
32 tially move from their niche into the circula-
33 tion crossing through endothelial cells from
34 vessel walls to the site of damage and ad-
35 here to the extracellular matrix (ECM) around
36 the wound. However, the trafficking of MSC
37 from their niche to target tissues is a com-
38 plex process. The migration process is affected
39 by chemokines, cytokines, growth factors and
40 mechanical factors such as shear stress, vascu-
41 lar cyclic stretching, and ECM adhesion [6].

42 Another important aspect of MSC is their

influence on different functions of surround- 43
ing cells in order to repair tissue damage by 44
promoting migration, adhesion and differenti- 45
ation, also determining cellular and biochemi- 46
cal changes in all phases of tissue damage [1]. 47
MSC also plays a role in immune processes 48
as they can respond to bacterial toxins and in- 49
flammatory cytokines. In this sense, it has 50
been described that MSC can be polarized in 51
vitro towards either pro- or anti-inflammatory 52
phenotypes, depending on the Toll-Like Re- 53
ceptor (TLR) ligand involved in their activa- 54
tion [7, 8]. In many infections TLR4 are ac- 55
tivated with lipopolysaccharides (LPS) which 56
are endotoxins present on the outer surface of 57
Gram Negative bacteria, and stimulate MSC 58
toward a pro-inflammatory phenotype, modu- 59
lating some of their functions [9]. Also, these 60
danger signals activate immune cells, and start 61
an appropriate host response with the aim to 62
reestablish homeostasis by recruiting them to 63
the site of injury. However, if the inflamma- 64
tory response turns out to be excessive, tis- 65
sue damage repairment may not be possible 66
[10]. Furthermore, TLRs are crucial in sensing 67
signals and switching immune responses from 68
MSC depending on the inflammatory state, 69
contributing in this way with the immunomod- 70
ulatory properties that MSC are well known to 71
have [11]. 72

73 Hemolytic uremic syndrome (HUS) is a dis-
74 ease caused by infections with enterohemor-
75 rhagic Gram-negative bacteria that produce
76 Shiga toxin (Stx). Once Stx accesses the cir-
77 culation, it interacts with a globotriaosylce-
78 ramide glycolipid receptor (Gb₃) in target cells
79 and this interaction leads to a cascade of events
80 that usually culminates with the inhibition of
81 protein synthesis and cell death. Endothelial
82 cell damage is a central event in the patho-
83 physiology of HUS and is the most important
84 factor of the microangiopathic process typi-
85 cally found in this disease [12]. In particular,

86 glomerular endothelial injury triggers a thrombotic microangiopathy leading to the formation of platelet and fibrin thrombi that occlude the microvasculature of the glomerulus, affecting renal function and resulting in acute renal failure. In addition to the toxic effects caused by the interaction of Stx with target cells, *in vivo* and *in vitro* evidence have demonstrated that LPS, present in all Gram-negative bacterial infections, potentiate endothelial cell damage by increasing susceptibility of these cells to the toxin [13, 14, 15]. Moreover, the presence of LPS triggers a strong inflammatory response, which can also contribute to endothelial dysfunction [16].

101 Taking into account that in many infections iPSC-MSC can be activated due to bacterial toxins and this can be decisive to reestablish homeostasis, the aim of this work was to investigate whether LPS and/or Stx treatments modify the iPSC-MSC secretory profile, and/or functions that could modulate the characteristic endothelial damage induced in the context of HUS.

110 **Materials and Methods**

111 *Cell cultures and treatments*

112 iPSC-MSC were obtained and differentiated as previously published [2]. These cells were maintained using alpha-MEM medium (Gibco, Ireland) supplemented with platelet lysate, 10 % of Penicillin-Streptomycin and glutamine (Gibco, Ireland). At 80 % of confluence, cells were trypsinized with 0.25 % of trypsin-EDTA (Gibco, Ireland). Human dermal Microvascular Endothelial Cells-1 (HMEC-1) were used to perform the experiments of endothelial damage. Cells were cultured at 37°C in a 5 % CO₂ humidified atmosphere using MCDB-131 medium (Gibco, Ireland) with phenol red and supplemented with 15 % fetal bovine serum (Na-

127 tocor, Argentina), penicillin (Gibco, Ireland), streptomycin (Gibco, Ireland), L-glutamine 10 mM (Gibco, Ireland), hydrocortisone 1 µg/mL (Sigma, USA) and endothelial cell growth supplement 20 µg/mL (Abcys, France). We set 4 treatment groups: Control (vehicle: only alpha-MEM), LPS (Sigma, USA, 0,5 ng/ml), Stx (Toxin Technology, USA, 20 ng/ml) and LPS+Stx. We exposed iPSC-MSCs and endothelial cells to Stx for 24 h. We used the type 2 variant of Stx (Stx2), as it is the most relevant in terms of epidemiology [17]. Also, as LPS is present in all Gram negative bacterial infections, and is the principal modulator of the inflammatory response, we use the combination of LPS+Stx for every experiment. Both LPS or Stx were added at the same time in LPS+Stx treatments. Also, Polymyxin B (Sigma, USA) was used in all treatments with Stx in order to avoid LPS contamination.

147 *Conditioned Media*

148 iPSC-MSC were seeded in alpha-MEM and treated with LPS and/or Stx during 24 h. Then, conditioned media (CM) were collected and incubated for 2 h with an anti-Stx antibody (anti-Stx2 variant from Toxin Technology, USA) to block the direct effect of Stx, or Polymyxin (Sigma, USA) to block the direct effect of LPS. In LPS+Stx CM, both anti-Stx and Polymyxin were used.

157 *Viability assays*

158 Cells were plated at subconfluency, treated for 24 h, and then gently washed to remove dead cells. After that, the remaining attached cells were fixed and dyed for 20 min using a solution of 0.1 % crystal violet in 20 % methanol. Then, the crystals were solubilized with 30 % acetic acid and measured with an ELISA detector at 540 nm. Several washes were done in order to eliminate the residual dye.

168 *Proliferation*

169 1 x 10⁵ iPSC-MSC cells were seeded in 96
170 well plates with LPS and/or Stx for 48 h at
171 37°C in 5 % CO₂. Then 0.5 μCi/well of 3H-
172 thymidine was added and incubated for an-
173 other 20 h. After that, cells were harvested,
174 scintillation fluid was added, and the radioac-
175 tive thymidine incorporated into DNA was
176 measured.

177 *Migration / Scratch assays*

178 iPSC-MSC or HMEC-1 cells were seeded to
179 confluence in 24-well plates (Jet Biofil) in the
180 corresponding culture media. In the case of
181 iPSC-MSC (migration assays), cells were in-
182 cubated for 24 h with media containing either
183 Control or toxins (LPS, Stx, LPS+Stx) before
184 scratch, while in HMEC-1 cells (wound re-
185 pair) the conditioned media from treated iPSC-
186 MSC was added immediately after doing the
187 scratch. Starting point (time 0) of the exper-
188 iment was defined as the moment when cells
189 were returned to the incubator, with an end
190 point of 18 h. Images were captured at both
191 instances with a Nikon Eclipse T5 100 micro-
192 scope and then analyzed with ImageJ software.
193 We used the freehand tool to manually draw
194 over the gap edges to determine the area of the
195 wound at time 0, 6 h (for iPSC-MSC) or 18 h
196 (for HMEC-1). The percentage of gap closure
197 was calculated as: [(gap area at 0 h - gap area
198 at x h)/gap area at 0 h] x100.

199 *Adhesion assay*

200 Adhesion of iPSC-MSC was evaluated on
201 96-well plates previously coated with 2 %
202 gelatin (40 min at room temperature, Sigma,
203 USA). Cells were first treated with vehicle
204 (Control), LPS, Stx and LPS+Stx and then col-
205 lected with trypsin, counted and seeded in the
206 gelatin-coated wells (20,000 cells/well). Cells
207 were allowed to attach for 15 min at 37°C

208 and stained with crystal violet solution. Im-
209 ages of adhered cells were captured using a
210 Nikon Eclipse T5 100 microscope and quanti-
211 fied with the ImageJ software using the count
212 cell option.

213 *Gb₃ measurement by Thin Layer Chromatog-*
214 *raphy (TLC)*

215 Gb₃ levels were detected by TLC and ana-
216 lyzed by densitometry. iPSC-MSC cells were
217 cultured in flasks and grown at 37°C in an at-
218 mosphere of 5 % CO₂ until cells were nearly
219 confluent. Cells were treated with Stx and/or
220 LPS as previously described. From each treat-
221 ment, total cells glycolipids were extracted ac-
222 cording to the method of Bligh and Dyer et. al
223 [18]. Briefly, 3 ml of chloroform:methanol 2:1
224 v/v were incorporated into the cells, and dur-
225 ing 15 min cells were incubated on ice. Two
226 ml of chloroform:water (1:1) were added and
227 centrifuged at 3,000 rpm for 5 min to separate
228 phases. The lower phase, corresponding to the
229 neutral glycolipid extract, was brought to dry-
230 ness and used for Gb₃ determination. One ml
231 of methanol and 0.1 ml of 1.0 M NaOH was
232 added to the dried residue, and incubated 16 h
233 at 37°C. Fractionated lipids were subjected to
234 TLC with a silica gel 60 aluminum plate previ-
235 ously activated by incubation 15 min at 100°C,
236 in a glass tank with a mixture of chloroform,
237 methanol, and water (65:35:8). To compare
238 quantities, a purified glycosphingolipid stan-
239 dard (0.5-1 and 2 μg) (Matreya, USA) was
240 also added to the plate. After the solvent front
241 reached the top of the plate, the gel matrix was
242 air dried and treated with a solution of orci-
243 nol, water and sulfuric acid (Acros Organics,
244 USA) to visualize the separated carbohydrate
245 and glycolipid components. The densitometric
246 analysis of Gb₃ bands was analyzed by Image
247 Quant 5.0 software. Values are expressed as
248 ng of Gb₃/10⁶ cells.

249 *ELISA assays*

250 Detection of TNF- α (BioLegend cat.
251 430205), IL-8 (BioLegend cat. 78141),
252 TGF- β (Biolegend, cat. 436707), and IL-10
253 (Biolegend, cat. 430601) from iPSC-MSC
254 were performed with ELISA kits, following
255 manufacturer's recommendations. Concentra-
256 tion results were obtained in pg/ml.

257 *Tubulogenesis assay*

258 Assays were performed on 96-well plates
259 coated with geltrex at 37°C for no less than
260 30 min. Approximately 15,000 HMEC-1
261 cells/100 μ l were seeded on coated wells using
262 EGM-2 media (Lonza, Switzerland) and incu-
263 bated overnight either with conditioned me-
264 dia from toxin-treated iPSC-MSC or vehicle
265 at 37 °C. Images of tube formation were cap-
266 tured the following day (24 h) using a Nikon
267 Eclipse T5 100 microscope followed by anal-
268 ysis on ImageJ software using the count the
269 branch points option obtained.

270 *Mass spectrometry (MS)*

271 LC-MS/MS (Liquid Chromatography with
272 tandem mass spectrometry) assays and MS
273 analysis on Conditioned Media of three tech-
274 nical replicates from vehicle (Control), LPS,
275 LPS+Stx and Stx-treated iPSC-MSC were
276 performed at the Proteomics Core Facility
277 CEQUIBIEM (University of Buenos Aires,
278 Buenos Aires, Argentina) following specifica-
279 tions detailed in La Greca et al, 2018 [19].
280 Briefly, peptides were reduced with dithiothre-
281 itol (DTT), precipitated with trichloroacetic
282 acid (TCA) and digested with trypsin. Ap-
283 proximately, 1 μ g of protein digests were an-
284 alyzed by nanoLC-MS/MS in a Thermo Sci-
285 entific QExactive Mass Spectrometer coupled
286 to a nanoHPLC EASY-nLC 1000. Data ac-
287 quisition and configuration for peptide iden-
288 tification were achieved with XCalibur 3.0.63
289 software and raw data produced was fed into

Proteome Discoverer software to classify iden- 290
tified peptides against Homo sapiens protein 291
sequences database (trypsin specificity) and 292
quantify abundance (area under the curve strat- 293
egy). 294

Bioinformatic analysis of MS data 295

Protein abundance obtained from Proteome 296
Discoverer in the form of area-based quantifi- 297
cation (area under the curve) [20] was em- 298
ployed for downstream bioinformatic analysis. 299
Technical replicates were collapsed and sam- 300
ples normalized by total area (total area per 301
sample/1000) using custom Python scripting. 302
Peptide abundance identified as ALBUMIN 303
(P02768) was excluded from further analy- 304
sis as it is most likely a residual contami- 305
nant from the platelet lysate used during iPSC- 306
MSC routine culture. The rest of the identified 307
proteins were clustered using a hierarchical- 308
based approach and plotted in a heatmap 309
using pheatmap package in R. In order to 310
aid visualization of identified proteins, Pro- 311
teinIDs were mapped to Gene Names using the 312
uniprotID converter (www.uniprot.org). On- 313
tological terms classified as “Biological pro- 314
cesses” (BPs) were determined using DOSE 315
[21] and clusterProfiler [22] packages keep- 316
ing only the top ten statistically signifi- 317
cant over-represented terms (p-value<0.01, q- 318
value<0.05). These over-represented BPs - 319
also called enriched- were determined by sta- 320
tistically testing (Fisher's exact test followed 321
by hypergeometric distribution test to evalu- 322
ate significance) the relationship between the 323
frequency of genes/proteins present in any 324
given term (observed or sample frequency) 325
and the frequency of genes/proteins annotated 326
to the same term (expected or background fre- 327
quency). Ultimately, this means that enriched 328
BPs showed observed frequency values higher 329
than their expected frequency for that term, 330

331 and the difference proved to be significant (p-
332 value<0.01).

333 *Statistical analysis*

334 Results are expressed as mean \pm S.E.M.
335 Significant differences (p<0,05) were iden-
336 tified using one way analysis of variance
337 (ANOVA) and Bonferroni's Multiple Test
338 Comparison using GraphPad software pack-
339 age (Prism 5.0 Version, San Diego, USA).

340 **Results**

341 *Gb₃-expressing iPSC-MSCs remained viable* 342 *after LPS and Stx treatments*

343 In order to establish the concentrations of
344 Stx and LPS to be used with iPSC-MSC
345 and endothelial cells we set two dose re-
346 sponse curves with different concentrations.
347 As a first step in determining the Stx concen-
348 tration needed to cause endothelial damage,
349 we treated Human Microvascular Endothelial
350 Cells (HMEC-1) with different doses of this
351 toxin, and measured the resultant viability af-
352 ter 24 h. As shown in Figure 1A, we found
353 that concentrations of 5, 10 and 20 ng/ml of
354 Stx were sufficient to cause endothelial cell
355 death in a dose dependent manner alone. LPS
356 did not show any additional toxic effect when
357 combined with Stx. Although LPS alone did
358 not induce HMEC-1 cytotoxicity, this concen-
359 tration of LPS was able to modulate endothe-
360 lial cell functions, by increasing ICAM-1 ex-
361 pression (Supp. Figure S1). In contrast to the
362 results observed in endothelial cells, none of
363 the concentrations of Stx or Stx in combination
364 with LPS (LPS+Stx) affected iPSC-MSC via-
365 bility (Figure 1B), or their proliferation mea-
366 sured by 3H-thymidine incorporation (Figure
367 1C).

368 In addition, because Stx did not affect iPSC-
369 MSC viability or proliferation levels, we de-
370 cided to determine the presence of the Gb₃

371 receptor in these cells. We obtained simi-
372 lar levels of Gb₃ expression on iPSC-MSC in
373 both Control and treated conditions (LPS, Stx,
374 and LPS+Stx) using thin layer chromatogra-
375 phy (Figure 1D).

376 These results indicate that even though
377 iPSC-MSC expresses the Stx receptor, treat-
378 ment with this toxin alone or in combina-
379 tion with LPS does not affect cell viability, in
380 contrast to what was observed for endothelial
381 cells.

382 *LPS induced a pro-inflammatory program on* 383 *iPSC-MSC but not Stx*

384 iPSC-MSC regulate their microenvironment
385 releasing different cytokines that can modu-
386 late biological processes in an autocrine or
387 paracrine way [23]. Moreover, inflammatory
388 signals released in many infections are asso-
389 ciated with migration, adhesion to the extra-
390 cellular matrix and many mechanisms near the
391 site of inflammation [9]. Therefore, in order
392 to determine the immunomodulatory contri-
393 bution of LPS- or Stx-treated iPSC-MSC, we
394 measured the release of the pro-inflammatory
395 cytokines IL-8, and TNF- α , and the anti-
396 inflammatory cytokines TGF- β and Il-10. As
397 shown in Figure 2A and B, only LPS signifi-
398 cantly increased the release of Il-8 and TNF-
399 α compared to Control cells. The addition of
400 Stx alone did not induce the release of IL-8
401 or TNF- α . Also, when iPSC-MSC were ex-
402 posed to LPS+Stx, they increased the produc-
403 tion of Il-8 and TNF- α compared to basal cells,
404 but TNF- α levels were lower compared to LPS
405 alone. Additionally, the presence of LPS, Stx
406 or LPS+Stx decreased significantly the levels
407 of the TGF- β compared to control cells. More-
408 over, both Il-10 and VEGF levels remained un-
409 detectable in all conditions (<15.6 and <31.3
410 pg/ml which are the lower detectable concen-
411 trations with EIISA kits respectively). These
412 results indicate that LPS polarizes iPSC-MSC

413 towards a pro-inflammatory phenotype, but
414 Stx does not contribute to this polarization de-
415 spite being a bacterial toxin.

416 *LPS and not Stx increased the migration of* 417 *iPSC-MSC*

418 It is known that in some inflammatory
419 pathologies, iPSC-MSC can respond to a wide
420 range of extracellular signals and modulate
421 some of their functions [9, 10]. In this sense,
422 we investigated the effect of LPS and Stx on
423 the capacity of iPSC-MSC to migrate after a
424 wound was performed. First, cells were in-
425 cubated with LPS, Stx or a combination of
426 both toxins for 24 h, and then a scratch was
427 performed mechanically across the cell mono-
428 layer. We observed that LPS treatment in-
429 creased the percentage of migration of iPSC-
430 MSC compared to control cells (Figure 3).
431 Conversely, Stx did not modify this function
432 showing similar migration as in basal condi-
433 tion. The combination of LPS+Stx increases
434 these percentages similar to LPS alone when
435 compared to control and Stx treated cells. In
436 conclusion, the inflammatory stimulus LPS in-
437 creases the migration of iPSC-MSC, whereas
438 Stx does not modify this effect.

439 *The combination of LPS+Stx augmented* 440 *iPSC-MSC capacity to adhere to extracellular* 441 *matrix*

442 The fact that iPSC-MSC migrate sensing
443 inflammatory signals involves an adhesion to
444 the extracellular matrix (ECM) in order to
445 reach the site of damage [24]. In this sense,
446 iPSC-MSC were used for measuring adhesion
447 to a substrate (gelatin), 24 h after incubation
448 with LPS, Stx or LPS+Stx. Treated cells
449 were harvested and settled on gelatine cov-
450 ered wells. After 15 minutes non-adhered cells
451 were eliminated by vigorous washing and rem-
452 nant gelatin-adhered cells were stained with
453 crystal violet and counted by microscopy. We

454 found that the treatment with LPS or Stx alone
455 did not alter adhesion to gelatin, although a
456 slight increase on adherent cells was found.
457 The combination of both toxins (LPS+Stx)
458 caused a statistically significant increase in
459 cell adhesion (Figure 4). This result suggests
460 that the effect of LPS on iPSC-MSC adhesion
461 to a gelatin matrix is potentiated by the pres-
462 ence of Stx.

463 *Conditioned media (CM) from iPSC-MSC ex-* 464 *posed to LPS+Stx decreased the capacity to re-* 465 *pair endothelial damage*

466 In order to investigate the effect of pro-
467 inflammatory iPSC-MSC on endothelial re-
468 pair, we performed a wound healing assay. For
469 this purpose, a scratch was performed across
470 a monolayer of endothelial cells HMEC-1.
471 Then, cells were treated with CM obtained
472 from iPSC-MSC that have been previously
473 treated or not with LPS, Stx, LPS+Stx for
474 24 h. Then, the percentage of endothelial
475 wound repair was measured. Figure 5A shows
476 that the presence of CM from LPS+Stx-treated
477 iPSC-MSC reduced wound closure compared
478 to non-treated iPSC-MSC CM. CM from LPS
479 and Stx alone-treated iPSC-MSC did not af-
480 fect this function. Moreover, none of the CM
481 affected the formation of new tubes on en-
482 dothelial cells (Figure 5B). These results in-
483 dicate that the effect of Stx and LPS treatment
484 on iPSC-MSC does not favor the repair of en-
485 dothelial damage.

486 *Analysis of proteins secreted by iPSC-MSC* 487 *treated with LPS and or Stx*

488 With the objective to explore the proteins se-
489 creted by iPSC-MSC in the CM after the treat-
490 ments with LPS and/or Stx, we performed a
491 proteomic analysis, as this technique allows
492 for the simultaneous identification of the pro-
493 teins present in any given sample, providing a

494 useful and fast method to assess relevant path-
495 ways or biological processes [25]. Thus, we
496 studied the expression levels of the proteins se-
497 creted to the CM by untreated cells (Control)
498 or cells treated with LPS, Stx and LPS+Stx
499 iPSC-MSC. Hierarchical clustering of protein
500 abundance data produced four different groups
501 revealing specific secretion profiles associated
502 with each experimental condition (Supp. Fig-
503 ure S2A). Functional analysis on clustered
504 data resulted in a set of over-represented onto-
505 logical terms (Supp. Figure S2B), in the form
506 of biological processes (BPs), that exposed im-
507 portant aspects of bacterial toxin treatment.

508 Gene ontology over representation analysis
509 on clustered data showed that some proteins
510 are more represented in the CM from iPSC-
511 MSC after treatment with LPS when com-
512 pared to control cells or with Stx and LPS+Stx
513 treatments. The proteins found in the CM
514 from iPSC-MSC treated with LPS but not with
515 the combination of both toxins are related
516 to BPs like “acute inflammatory response”,
517 “platelet degranulation”, “regulation of fibrin-
518 olysis” and “extracellular matrix organiza-
519 tion” (e.g. SERPINE1, AHSG1, FN, THBS1,
520 PLG, PTX3 and CCN2 (Figure 6A)), in line
521 with results obtained in Figure 2 where LPS
522 polarized iPSC-MSC to a pro-inflammatory
523 profile increasing migration and adhesion to
524 extracellular matrix (Figure 3 and 4).

525 Furthermore, LPS+Stx increased the ex-
526 pression of proteins related to BP “IL-12 me-
527 diated signaling pathway”, “endopeptidase ac-
528 tivity” and “actin filament organization” (e.g.
529 PPIA) (Figure 6B). These proteins can be as-
530 sociated with Figure 5, where a decreased ca-
531 pacity of wound closure was observed in en-
532 dothelial cells incubated with the iPSC-MS
533 treated with LPS+Stx.

534 Discussion

535 Immune responses against bacterial toxins
536 are crucial to resolve infectious pathologies.
537 Usually, different cell types are recruited to re-
538 spond and participate in order to reestablish
539 the altered homeostasis. The mechanisms in-
540 volved in these processes include the secre-
541 tion of a wide range of cytokines to the envi-
542 ronment in order to attract different cells that
543 can positively or negatively modulate tissue
544 damage. Mesenchymal stem cells (MSC) are
545 known to participate in these processes secre-
546 ting cytokines that are involved in many mech-
547 anisms with the aim of restoring tissue in-
548 jury, often present due to infections [9]. In
549 this sense, host immune cells can recognize
550 some bacterial toxins such as LPS and mount
551 defenses to clear pathogens, releasing pro-
552 inflammatory cytokines that contribute to ac-
553 tivate immune and non immune cells with the
554 objective to restore homeostasis. TLR4 rec-
555 ognizes LPS, and cell activation through this
556 receptor leads to profound cellular and sys-
557 temic responses that mobilize innate and adap-
558 tive host immune cells [26]. Another bacte-
559 rial toxin that participates in inflammatory pro-
560 cesses is Shiga toxin (Stx). This multifunc-
561 tional toxin is capable of inducing cell stress
562 and activating innate immune responses that
563 may lead to inflammation increasing the sever-
564 ity of organ injury in HUS patients [27]. Tak-
565 ing this into account, we investigated the effect
566 of LPS and/or Stx on iPSC-MSC. Particularly,
567 in this work it was studied the induction of
568 secreted soluble factors from iPSC-MSC ex-
569 posed to both bacterial toxins and their possi-
570 ble contribution on endothelial damage.

571 To the best of our knowledge, this is the
572 first report describing expression of Gb₃ in
573 iPSC-MSC. This result is relevant for featur-
574 ing iPSC-MSC as direct potential cellular tar-
575 gets for Stx. It has been demonstrated that

576 Gb3 mediates the entrance of Stx to target
577 cells, e.g. endothelial cells, generally causing
578 cell death [28]. However, we did not observe
579 any toxic effect on iPSC-MSC after incubation
580 with Stx, in contrast to what happens with en-
581 dothelial cells. In line with this result, Gee-
582 len et. al. showed that although monocytes
583 express a receptor for Stx, they do not show
584 any cytotoxic effect after incubation with Stx
585 [29], indicating that cell death is not the only
586 possible result after Stx interacts with its re-
587 ceptor. Furthermore, we observed that iPSC-
588 MSC cultured with LPS increased their capac-
589 ity to migrate and adhere to extracellular ma-
590 trix (ECM) proteins. Interestingly, when we
591 measured the ability of iPSC-MSC to attach
592 to the ECM, we observed an additive effect
593 between LPS and Stx in this function, prob-
594 ably reflecting the physiopathological events
595 that occur in a context of infection with a Stx-
596 producing *E. coli* in HUS. These functional
597 results (Figure 3 and 4) were consistent with
598 the secreted proteins obtained in the proteomic
599 analysis from the CM of iPSC-MSC treated
600 with LPS. The results showed that iPSC-MSC
601 contributed to creating an inflammatory envi-
602 ronment as we observed in ELISA assays (IL-
603 8 and TNF- α increments, Figure 2) but also
604 in the proteomic analysis. For example SER-
605 PINE1 is involved in acute inflammatory re-
606 sponses as is described in hepatocytes, mono-
607 cytes, macrophages and bronchiolar cells [30],
608 AHSG1 is a protein associated with inflam-
609 mation and chronic diseases such as endotox-
610 emia and sepsis [31], THBS1 represents a po-
611 tent pro-inflammatory signal for macrophages,
612 and is also produced by them [32], PLG is
613 an enzyme with a crucial role in inflamma-
614 tion and coagulation [33], FN is a ubiquitous
615 and essential component of the extracellular
616 matrix that participates in many events related
617 to cell migration and adhesion [34] and PTX3
618 is a prototypic soluble pattern recognition re-

619 ceptor, expressed at sites of inflammation and
620 involved in regulation of tissue homeostasis.
621 Systemic levels of PTX3 increase in many (but
622 not all) immune-mediated inflammatory condi-
623 tions [35]. All these proteins were found
624 in higher quantities in the CM of iPSC-MSC
625 treated with LPS, in accordance with an in-
626 duction of the pro-inflammatory program that
627 these cells acquired.

628 To the best of our knowledge, this is the
629 first report describing the expression of Gb₃ in
630 iPSC-MSC. This result is relevant for featur-
631 ing iPSC-MSC as direct potential cellular tar-
632 gets for Stx. It has been demonstrated that Gb3
633 mediates the entrance of Stx to target cells, e.g.
634 endothelial cells, generally causing cell death
635 [28]. However, we did not observe any toxic
636 effect on iPSC-MSC after incubation with Stx,
637 in contrast to what happens with endothelial
638 cells. In line with this result, Monnens et.
639 al. [29] showed that although monocytes ex-
640 press a receptor for Stx, they do not show any
641 cytotoxic effect after incubation with Stx, in-
642 dicated that cell death is not the only possi-
643 ble result after Stx interacts with its recep-
644 tor. Furthermore, we observed that iPSC-MSC
645 stimulated with LPS increased their capacity
646 to migrate and adhere to extracellular matrix
647 (ECM) proteins. Interestingly, when we mea-
648 sured the ability of iPSC-MSC to attach to
649 the ECM, we observed an additive effect be-
650 tween LPS and Stx in this function, probably
651 reflecting the physiopathological events that
652 occur in a context of infection with a Stx-
653 producing *E. coli* in HUS. These functional
654 results (Figure 3 and 4) were consistent with
655 the secreted proteins obtained in the proteomic
656 analysis from the CM of iPSC-MSC treated
657 with LPS. The results showed that iPSC-MSC
658 contributed to creating an inflammatory envi-
659 ronment as we observed in ELISA assays (IL-
660 8 and TNF- α increments, Figure 2) but also
661 in the proteomic analysis. For example SER-

662 PINE1 is involved in acute inflammatory re-
663 sponses as is described in hepatocytes, mono-
664 cytes, macrophages and bronchiolar cells [30],
665 AHSG1 is a protein associated with inflam-
666 mation and chronic diseases such as endotox-
667 emia and sepsis [31], THBS1 represents a po-
668 tent pro-inflammatory signal for macrophages,
669 and is also produced by them [32], PLG is
670 an enzyme with a crucial role in inflamma-
671 tion and coagulation [33], FN is a ubiquitous
672 and essential component of the extracellular
673 matrix that participates in many events related
674 to cell migration and adhesion [34] and PTX3
675 is a prototypic soluble pattern recognition re-
676 ceptor, expressed at sites of inflammation and
677 involved in regulation of tissue homeostasis.
678 Systemic levels of PTX3 increase in many (but
679 not all) immune-mediated inflammatory con-
680 ditions [35]. All these proteins were found
681 in higher quantities in the CM of iPSC-MSC
682 treated with LPS, in accordance with an in-
683 duction of the pro-inflammatory program that
684 these cells acquired.

685 Another fact observed in this work was
686 that Stx treatment did not modulate any of
687 the iPSC-MSC functions assayed, and did not
688 generate a pro-inflammatory profile as LPS
689 did, indicating that LPS is the main inducer of
690 a pro-inflammatory profile in these cells in a
691 context of HUS.

692 Although we did not observe an increase in
693 the percentage of wound repair in endothelial
694 cells exposed to CM from iPSC-MSC treated
695 with LPS+Stx, the combination of both tox-
696 ins decreased the capacity of iPSC-MSC to
697 restore the endothelial damage and also, did
698 not modify the mechanism of new tube for-
699 mation. We hypothesize that the treatments
700 with LPS+Stx on iPSC-MSC induce the re-
701 lease of some factors that decrease the capac-
702 ity of endothelial cells to repair a wound. In
703 this sense, in the proteomic analysis we found
704 that the use of LPS+Stx in iPSC-MSC, in-

duced the release of proteins related to the BP 705
of “IL-12 mediated signalling pathway” such 706
as PPIA, which is reported to promote apop- 707
tosis in endothelial cells and chemotaxis in in- 708
flammatory cells [36]. As Wong and Water- 709
man et.al described in a previous work, we 710
can speculate that activation of TLR4 in iPSC- 711
MSC due to LPS resulted in the secretion of 712
pro-inflammatory factors in the CM that are 713
important for early injury responses, like mi- 714
gration and cell adhesion to ECM, but not to 715
resolve tissue damage [9]. However, these 716
mechanisms could prepare the microenviron- 717
ment for later iPSC-MSC anti-inflammatory 718
responses that could facilitate the restoration 719
of tissue injury. This second response could 720
be possible as it is known that MSC can pro- 721
mote or inhibit immune responses due to their 722
immunomodulatory properties, determined by 723
the strength of the inflammatory milieu ([10], 724
Figure 6C). In this sense, proteomics results 725
in concordance with the Biological Processes 726
(BPs) “platelet degranulation”, suggests that 727
soluble mediators released after LPS treatment 728
could bring platelets into the picture. A cru- 729
cial factor for endothelial growth and repair is 730
vascular endothelial growth factor (VEGF). It 731
is known that platelets can participate in the 732
restoration of tissue (i.e. endothelial) dam- 733
age interacting with iPSC-MSC through the 734
release of different factors [37]. Degranula- 735
tion of platelets by factors released by treated 736
iPSC-MSC may be of particular interest for 737
endothelial repair, considering that platelets 738
produce VEGF in many physiological situa- 739
tions, such as inflammation [38]. Although 740
in our experimental model we did not include 741
these cells, future research will be done in this 742
way. It should be noted that levels of VEGF in 743
ELISA assays from CM of treated iPSC-MSC 744
were undetectable, even though these cells are 745
known to produce and release this endothe- 746
lial growth factor [39]. The release of VEGF 747

748 through the exosome pathway, could be an-
749 other mechanism to explain the lack of detec-
750 tion of this growth factor in our analyses [40],
751 as our protocol for sample preparation for pro-
752 teomic analysis did not break these vesicles
753 [19].

754 In conclusion, in this work we showed that
755 LPS generates an inflammatory program in
756 iPSC-MSC that induces migration and adhe-
757 sion to proteins present in ECM and these re-
758 sults was in concordance with the secretion
759 of different proteins observed in ELISAs and
760 proteomic assays. Stx alone did not induce
761 inflammatory responses, even though iPSC-
762 MSC expresses Gb₃, but when combined with
763 LPS, it decreased the capacity of endothelial
764 cells to resolve a wound. The results observed
765 in this work helps understand the role of iPSC-
766 MSC in tissue regeneration, indicating that the
767 immune context generated from these cells in
768 response to a particular bacterial toxin should
769 be taken into account.

770 Data Availability

771 All LC-MS/MS raw data will be publicly
772 available at Mass Spectrometry Interactive
773 Virtual Environment (MassIVE) upon publica-
774 tion of the manuscript.

775 Acknowledgments

776 The authors would like to thank LIAN
777 (FLENI-CONICET) for allowing us to use
778 laboratory facilities to perform many of the ex-
779 periments from this work.

780 Declaration of Interests

781 The authors declare no competing interests.

References

- [1] Wang Y, Chen X, Cao W, Shi Y. Plasticity of mesenchymal stem cells in immunomodulation: pathological and therapeutic implications. *Nat Immunol.* 2014 Nov;15(11):1009–16.
- [2] Luzzani C, Neiman G, Garate X, Questa M, Solari C, Fernandez Espinosa D, et al. A therapy-grade protocol for differentiation of pluripotent stem cells into mesenchymal stem cells using platelet lysate as supplement. *Stem Cell Res Ther.* 2015 Jan;6:6.
- [3] Cantinieaux D, Quertainmont R, Blacher S, Rossi L, Wanet T, Noël A, et al. Conditioned medium from bone marrow-derived mesenchymal stem cells improves recovery after spinal cord injury in rats: an original strategy to avoid cell transplantation. *PLoS One.* 2013;8(8):e69515.
- [4] Prockop DJ. Repair of tissues by adult stem/progenitor cells (MSCs): controversies, myths, and changing paradigms. *Mol Ther.* 2009 Jun;17(6):939–46.
- [5] Fu X, Liu G, Halim A, Ju Y, Luo Q, Song, et al. Mesenchymal Stem Cell Migration and Tissue Repair. *Cells.* 2019 07;8(8).
- [6] Sacchetti B, Funari A, Michienzi S, Di Cesare S, Piersanti S, Saggio I, et al. Self-renewing osteoprogenitors in bone marrow sinusoids can organize a hematopoietic microenvironment. *Cell.* 2007 Oct;131(2):324–36.
- [7] Walter J, Ware LB, Matthay MA. Mesenchymal stem cells: mechanisms of potential therapeutic benefit in ARDS and sepsis. *Lancet Respir Med.* 2014 Dec;2(12):1016–26.
- [8] Lombardo E, van der Poll T, DelaRosa O, Dalemans W. Mesenchymal stem cells as a therapeutic tool to treat sepsis. *World J Stem Cells.* 2015 Mar;7(2):368–79.
- [9] Kurte M, Vega-Letter AM, Luz-Crawford P, Djouad F, Noël D, Khoury M, et al. Time-dependent LPS exposure commands MSC immunoplasticity through TLR4 activation leading to opposite therapeutic outcome in EAE. *Stem Cell Res Ther.* 2020 09;11(1):416.
- [10] Waterman RS, Tomchuck SL, Henkle SL, Betancourt AM. A new mesenchymal stem cell (MSC) paradigm: polarization into a pro-inflammatory MSC1 or an Immunosuppressive MSC2 phenotype. *PLoS One.* 2010 Apr;5(4):e10088.
- [11] Jiang W, Xu J. Immune modulation by mesenchymal stem cells. *Cell Prolif.* 2020 Jan;53(1):e12712.

- [12] Joseph A, Cointe A, Mariani Kurkdjian P, Rafat C, Hertig A. Shiga Toxin-Associated Hemolytic Uremic Syndrome: A Narrative Review. *Toxins* (Basel). 2020 01;12(2).
- [13] Karmali MA. Infection by Shiga toxin-producing *Escherichia coli*: an overview. *Mol Biotechnol*. 2004 Feb;26(2):117–22.
- [14] Forsyth KD, Simpson AC, Fitzpatrick MM, Barratt TM, Levinsky RJ. Neutrophil-mediated endothelial injury in haemolytic uraemic syndrome. *Lancet*. 1989 Aug;2(8660):411–4.
- [15] Boyce TG, Swerdlow DL, Griffin PM. *Escherichia coli* O157:H7 and the hemolytic-uremic syndrome. *N Engl J Med*. 1995 Aug;333(6):364–8.
- [16] Exeni RA, Fernández GC, Palermo MS. Role of polymorphonuclear leukocytes in the pathophysiology of typical hemolytic uremic syndrome. *ScientificWorldJournal*. 2007 Aug;7:1155–64.
- [17] Reyes-Rodriguez NE, Reyes-Rodriguez NE, Barba-León J, Navarro-Ocaña A, Vega-Sanchez V, Anda FRGD, et al. Serotypes and Stx2 subtyping of Shiga toxin producing *Escherichia coli* isolates from cattle carcasses and feces. *Revista Mexicana de Ciencias Pecuarias*. 2020;11(4):1030–1044. Available from: <https://cienciaspecuarias.inifap.gob.mx/index.php/Pecuarias/article/view/5049>.
- [18] BLIGH EG, DYER WJ. A rapid method of total lipid extraction and purification. *Can J Biochem Physiol*. 1959 Aug;37(8):911–7.
- [19] La Greca A, Solari C, Furmento V, Lombardi A, Biani MC, Aban C, et al. Extracellular vesicles from pluripotent stem cell-derived mesenchymal stem cells acquire a stromal modulatory proteomic pattern during differentiation. *Exp Mol Med*. 2018 09;50(9):1–12.
- [20] Ning K, Fermin D, Nesvizhskii AI. Comparative analysis of different label-free mass spectrometry based protein abundance estimates and their correlation with RNA-Seq gene expression data. *J Proteome Res*. 2012 Apr;11(4):2261–71.
- [21] Yu G, Wang LG, Yan GR, He QY. DOSE: an R/Bioconductor package for disease ontology semantic and enrichment analysis. *Bioinformatics*. 2015 Feb;31(4):608–9.
- [22] Yu G, Wang LG, Han Y, He QY. clusterProfiler: an R package for comparing biological themes among gene clusters. *OMICS*. 2012 May;16(5):284–7.
- [23] Al Bahrawy M, Ghaffar K, Gamal A, El-Sayed K, Iacono V. Effect of Inflammation on Gingival Mesenchymal Stem/Progenitor Cells' Proliferation and Migration through Microperforated Membranes: An In Vitro Study. *Stem Cells Int*. 2020;2020:5373418.
- [24] Noronha NdC, Mizukami A, Caliári-Oliveira C, Cominal JG, Rocha JLM, Covas DT, et al. Priming approaches to improve the efficacy of mesenchymal stromal cell-based therapies. *Stem Cell Res Ther*. 2019 05;10(1):131.
- [25] Aslam B, Basit M, Nisar MA, Khurshid M, Rasool MH. Proteomics: Technologies and Their Applications. *J Chromatogr Sci*. 2017 02;55(2):182–196.
- [26] Vijay K. Toll-like receptors in immunity and inflammatory diseases: Past, present, and future. *Int Immunopharmacol*. 2018 Jun;59:391–412.
- [27] Lee MS, Tesh VL. Roles of Shiga Toxins in Immunopathology. *Toxins* (Basel). 2019 04;11(4).
- [28] Pijpers AHJM, Setten PAV, Heuvel LPWJVD, Assmann KJM, Dijkman HBPM, Pennings AHM, et al. Verocytotoxin-induced apoptosis of human microvascular endothelial cells. *J Am Soc Nephrol*. 2001 Apr;12(4):767–778.
- [29] Geelen JM, van der Velden TJAM, van den Heuvel LPWJ, Monnens LAH. Interactions of Shiga-like toxin with human peripheral blood monocytes. *Pediatr Nephrol*. 2007 Aug;22(8):1181–7.
- [30] Lee J, Lu Y, Oshins R, West J, Moneypenny CG, Han K, et al. Alpha 1 Antitrypsin-Deficient Macrophages Have Impaired Efferocytosis of Apoptotic Neutrophils. *Front Immunol*. 2020;11:574410.
- [31] Lin YH, Zhu J, Meijer S, Franc V, Heck AJR. Glycoproteogenomics: A Frequent Gene Polymorphism Affects the Glycosylation Pattern of the Human Serum Fetuin/ α -2-HS-Glycoprotein. *Mol Cell Proteomics*. 2019 08;18(8):1479–1490.
- [32] Xiao M, Zhang J, Chen W, Chen W. M1-like tumor-associated macrophages activated by exosome-transferred THBS1 promote malignant migration in oral squamous cell carcinoma. *J Exp Clin Cancer Res*. 2018 Jul;37(1):143.
- [33] Baker SK, Strickland S. A critical role for plasminogen in inflammation. *J Exp Med*. 2020 04;217(4).
- [34] Bazan-Socha S, Kuczia P, Potaczek DP, Mastalerz L, Cybulska A, Zareba L, et al. Increased blood levels of cellular fibronectin in asthma: Relation to the asthma severity, inflammation, and prothrombotic blood alterations. *Respir Med*. 2018

- 08;141:64–71.
- [35] Ramirez GA, Rovere-Querini P, Blasi M, Sartorelli S, Di Chio MC, Baldini M, et al. PTX3 Intercepts Vascular Inflammation in Systemic Immune-Mediated Diseases. *Front Immunol.* 2019;10:1135.
 - [36] Xie Y, Li X, Ge J. Cyclophilin A-FoxO1 signaling pathway in endothelial cell apoptosis. *Cell Signal.* 2019 09;61:57–65.
 - [37] Qiao J, An N, Ouyang X. Quantification of growth factors in different platelet concentrates. *Platelets.* 2017 Dec;28(8):774–778.
 - [38] Peterson JE, Zurakowski D, Italiano JE Jr, Michel LV, Connors S, Oenick M, et al. VEGF, PF4 and PDGF are elevated in platelets of colorectal cancer patients. *Angiogenesis.* 2012 Jun;15(2):265–73.
 - [39] Yang Y, Hu S, Xu X, Li J, Liu A, Han J, et al. The Vascular Endothelial Growth Factors-Expressing Character of Mesenchymal Stem Cells Plays a Positive Role in Treatment of Acute Lung Injury In Vivo. *Mediators Inflamm.* 2016;2016:2347938.
 - [40] Olejarz W, Kubiak-Tomaszewska G, Chrzanowska A, Lorenc T. Exosomes in Angiogenesis and Anti-angiogenic Therapy in Cancers. *Int J Mol Sci.* 2020 Aug;21(16).

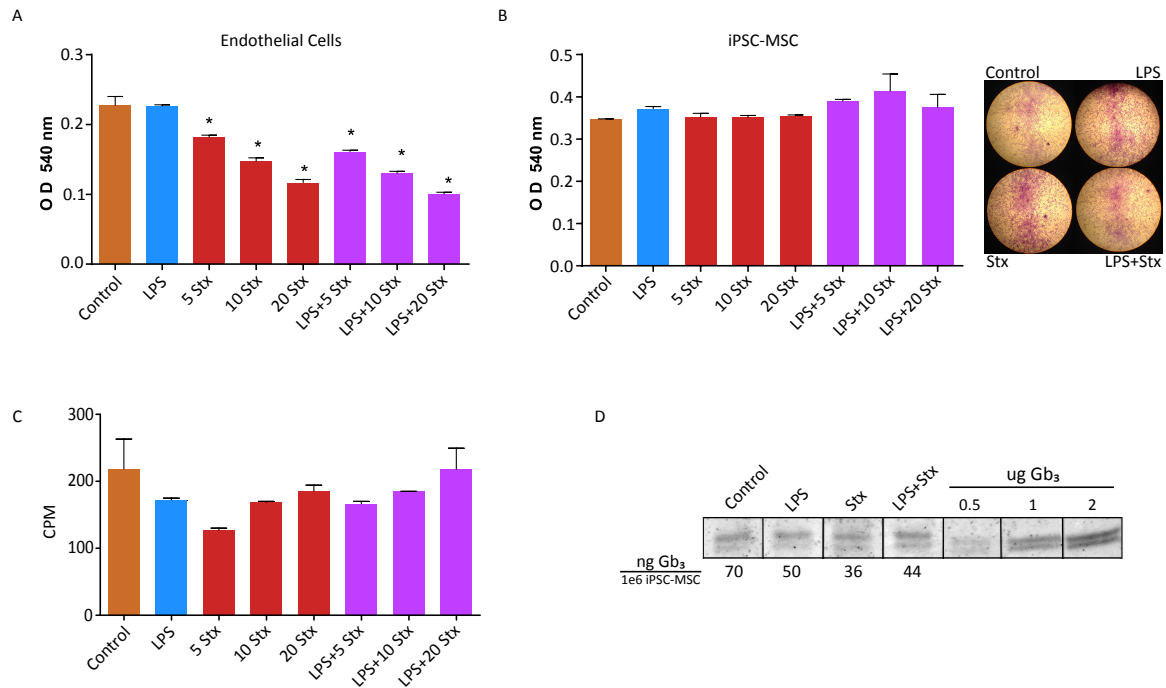


Figure 1: Effect of Stx and LPS on the viability of endothelial cells, iPSC-MSC and its Gb₃ expression. (A) Viability of HMEC-1 treated with LPS (500 ng/ml), alone or in combination with different Stx concentrations (5-20 ng/ml) were measured at 540 nm, and optic density (O.D.) from crystal violet were represented from each treatment. (B) Viability of iPSC-MSC treated with LPS (500 ng/ml), alone or in combination with different Stx concentrations (5-20 ng/ml) were measured at 540 nm, and optic density (O.D.) from crystal violet were represented from each treatment. Representative microphotographs depicting iPSC-MSC cultures are shown in the right panel (x10). (C) Proliferation was measured by 3H-thymidine incorporation on control and treated iPSC-MSC, 72 h post stimulus. Counts per minute (CPM) are shown. (D) Thin Layer Chromatography (TLC) assays performed in Control and treated iPSC-MSC to measure the expression of Gb₃ receptor compared to known Gb₃ standards (0.5, 1 and 2 μg). Gb₃ quantification (ng Gb₃/1e⁶ iPSC-MSC) is shown below each treatment column. Results were expressed as mean ± S.E.M. n = 12–18 per group; *P<0.05.

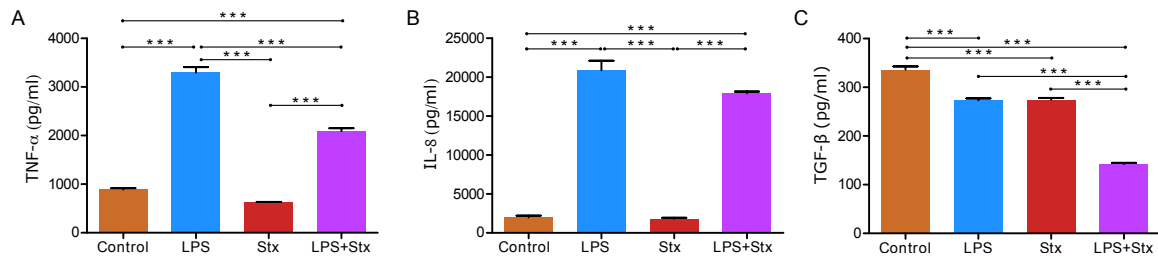


Figure 2: **Inflammatory cytokines are produced by iPSC-MSC in contact with LPS. Stx did not have this effect.** iPSC-MSC were treated with LPS and/or Stx for 24 h and then secreted TNF- α (A), IL-8 (B) and TGF- β (C) were determined using ELISA kits. Results were expressed as mean \pm S.E.M. n = 3 per group; ***P<0.001.

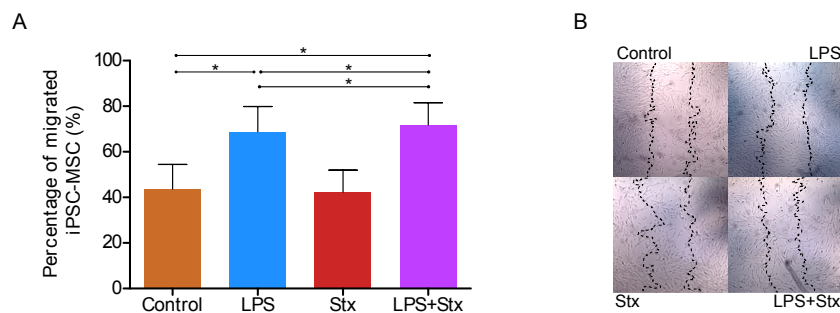


Figure 3: **LPS increased iPSC-MSC migration and Stx did not modulate this function.** Percentage of migrated area from LPS and/or Stx treated or Control iPSC-MSC after 6 h post-scratch over the monolayer of the cells. Representative microphotographs are shown for each treatment in the right panel. The discontinuous line represents the wound at time 0. Results were expressed as mean \pm S.E.M. n = 8 per group; *P<0.05.

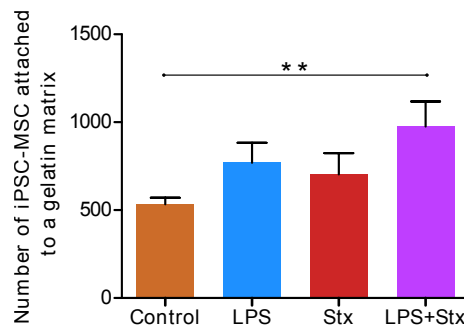


Figure 4: **LPS+Stx increased in iPSC-MSC the adhesion to gelatin.** Adhered iPSC-MSC to gelatin after 24 h of being treated with LPS and/or Stx. Results were expressed as mean \pm S.E.M. n = 4 per group; **P<0.01.

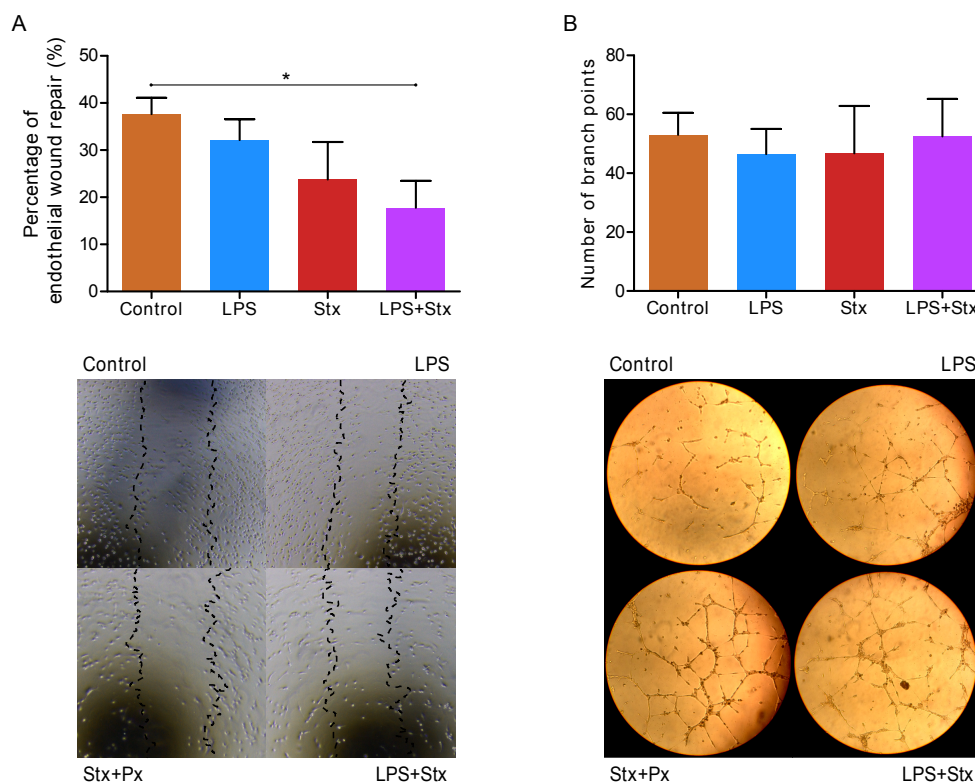


Figure 5: **LPS+Stx decreased in iPSC-MSC repair mechanisms in endothelial cells.** Conditioned media (CM) from iPSC-MSC treated with LPS and/or Stx were added to endothelial cells for (A) wound healing assay (percentage of endothelial wound repair is shown and representatives microphotographs are shown) (B) tubulogenesis assay (number of branch points is shown and representatives microphotographs are shown). Results were expressed as mean \pm S.E.M. n = 8 per group; *P<0.05.

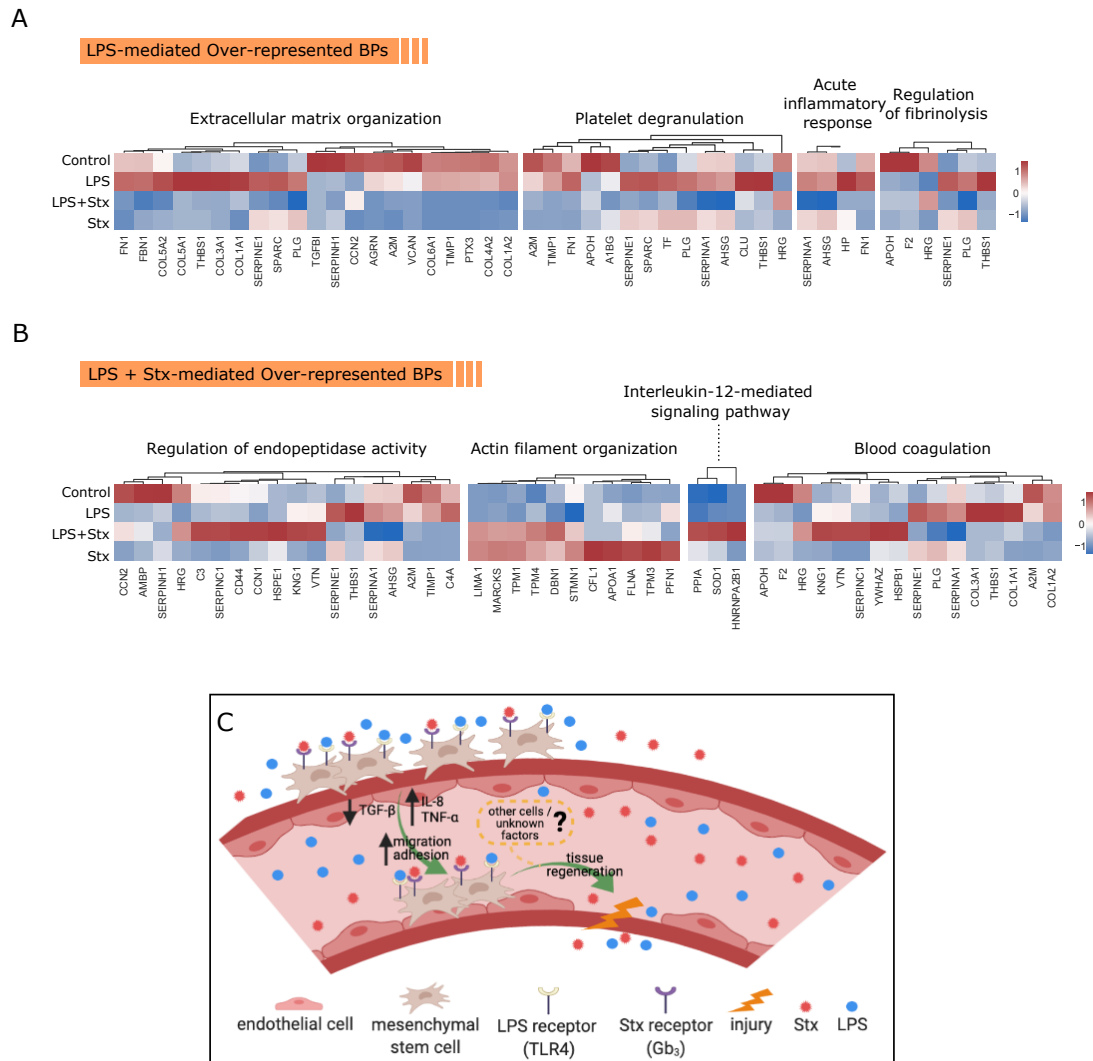


Figure 6: **Protein abundance levels found in over-represented biological processes from toxin-treated iPSC-MSC.** Comparative protein levels among treatments for biological processes found predominantly in (A) clusters 3 and 4 and in (B) clusters 1 and 2. Heatmap was plotted using scaled (z-score) normalized areas in which red color indicates higher abundance while blue represents low abundance. Dendrograms on top of heatmaps reflect hierarchical clustering of proteins. (C) Schematic representation of a segment of a blood vessel and the events triggered by LPS and Stx treatments focusing on MSC response. Created with BioRender (biorender.com).

Supplemental information

Supp. Figure S1. LPS-dependent ICAM-1 expression in endothelial cells. Mean fluorescence intensity (MFI) of ICAM-1 is shown for endothelial cells (HMEC-1) treated or not with 100 ng/ml LPS for 2 h. Results were expressed as mean \pm S.E.M. n = 6 per group; **P<0.01.

Supp. Figure S2. Biological processes related to proteins identified in CM of iPSC-MSC reflect the migration, adhesion to substrate and immune response induced by toxins. (A) Heatmap shows normalized levels of proteins from collapsed technical replicates identified by proteomic analysis in the CM of untreated (Control, n=3) iPSC-MSC or treated with LPS (n=3), Stx (n=3) and LPS+Stx (n=3). Dendrograms represent the unsupervised euclidean (method) clustering of peptides (left). Names of identified proteins are shown to the right of the plot. (B) Overrepresented biological processes related to clustered proteins from (A) ordered by gene ratio (percentage of identified proteins in an ontology term). Size of spheres denotes the number of proteins contained in each process and color features the statistical significance of the algorithm represented by the adjusted p-value (Benjamini-Hochberg).